Finite Element Modeling of Thin Conductors in Frequency-Domain

Jonathan Velasco[1], François Henrotte[1,2], and Christophe Geuzaine[1],
[1]Department Electrical Engineering and Computer Science (ACE), Institut Montefiore, University of Liège, Belgium
[2]Catholic University of Louvain (UCL), EPL-iMMC-MEMA, Louvain, Belgium
jonathan.velasco@uliege.be

This paper describes a technique that allows representing thin wires in finite element models very efficiently and accurately by idealized line elements. The approach exploits the analytical solution of the problem of the wire taken in isolation to correct the finite element solution of the problem of the idealized wire with vanishing radius. The method is validated in the 2D magnetodynamics frequency-domain case for systems of parallel wires.

***Index Terms*—Thin wire, analytical approximation, conducting domains, local correction, eddy currents, skin depth, proximity effect**

I. Introduction

Electrical conductors are ubiquitous in electromagnetic devices. They come in various shapes like wires, twisted wires, coaxial cables, busbars, etc, which we shall call *thin wires* in this paper to emphasize their large axial to transversal dimension ratio. The effect of such thin wires in systems is two-fold: It consists in an impedance Z_w in an electric or electronic circuit, and in a radiated field $\mathbf{b}_w$.

The radiated field $\mathbf{b}_w$ may affect distant parts of the systems. As it however depends only, outside the wire, on the net current I_w flowing in the wire, the details of the internal electromagnetic field distribution are decoupled from the rest of the system, provided the net current I_w is known. Therefore, they do not need to be resolved explicitly.

Moreover, the geometry of those thin wires, as they are an accessory and often flexible, is in general not accurately determined. A quick and versatile solution to integrate such components in the CAD of the studied system would be very practical and useful.

This paper presents a technique to represent thin wires with an arbitrary internal structure in FE models a sequence of edges of the mesh, avoiding so a dense and costly discretization of the thin conduction regions, but still accounting for the (quasi) exact impedance of the wire by means of a correction based on available analytical solutions.

Although the principles of the method are explained in this paper in the case of a 2D $\mathbf{a}-v$ eddy current formulation in the frequency domain, where the thin conductors are replaced by points, the proposed technique is rather general. In 3D, the thin conductors would be represented by a set of consecutive edges of the mesh and the principle of the method still applies in the same manner.

II. $\mathbf{a}-v$ formulation with normal conductors

For the sake of clarity, the technique is demonstrated in this paper in the 2D time-harmonic case with an homogeneous Dirichlet boundary condition $\mathbf{a}=0$ on the whole boundary $\partial\Omega$, so as to leave aside specific issues (gauging, Neumann type boundary condition, voltage sources, time stepping schemes) that do not affect the main ideas of the proposed correction technique.

The weak form of the $\mathbf{a}-v$ formulation for the eddy current problems with normal massive conductors is first recalled. Let the conducting region

$$\Omega_c = \bigcup_k \Omega_{ck}$$

be the union of the conductors Ω_{ck} with cross section area A_k, and Ω_c^C be the complementary non-conduction regions. The computation domain is thus $\Omega=\Omega_c^C\cup\Omega_c$. The conductors Ω_{ck} are supplied with a sinusoidal current source $I_k=\hat{I}_k\cos(\omega t+\theta_k)$, where $\hat{I}_k$ is the current peak value, ω the angular frequency, and θ_k the phase shift.

In 2D, the magnetic vector potential field is discretized as

$$\mathbf{a}=\sum_n a_n\alpha_n\mathbf{e}_z,$$

where α_n are nodal shape functions and $\mathbf{e}_z$ is the unit vector perpendicular to the domain of analysis Ω. The gradient of the scalar electric potential, on the other hand, is discretized as

$$-\operatorname{grad} v=\sum_k(\Delta v)_k\beta_k\mathbf{e}_z,$$

where $(\Delta v)_k$ are the voltage drop per unit length in z direction imposed to the conductors Ω_{ck}, and β_k are the corresponding regionwise constant shape functions.

With these notations, the $\mathbf{a}-v$ formulation writes in weak form as a set of field equations associated with the free nodes of the mesh

$$\big(\nu\operatorname{curl}\mathbf{a},\operatorname{curl}(\alpha_n\mathbf{e}_z)\big)_\Omega + \big(\sigma(\imath\omega\mathbf{a}+\operatorname{grad} v),\alpha_n\mathbf{e}_z\big)_{\Omega_c}=0,\quad\forall\alpha_n\in A(\Omega),\quad(1)$$

and one current control equation per conductor

$$\big(-\sigma(\imath\omega\mathbf{a}+\operatorname{grad} v),\beta_k\mathbf{e}_z\big)_{\Omega_c}=I_k,\quad\forall\beta_k\in V(\Omega),\quad(2)$$

where ν is the magnetic reluctivity, and σ the electric conductivity. In (1-2), $A(\Omega)$ and $V(\Omega)$ are appropriate function spaces

Manuscript received August 18, 2019; revised August XX, XXXX. Corresponding author: J. Velasco (email: jonathan.velasco@uliege.be).

according to the discretization and the boundary conditions of the problem, Note that $(\cdot,\cdot)_\Omega$ denotes the the volume integral over Ω of the dot product of its vector field arguments.

Before proceeding with the geometrical thin wire approximation, the definition of the impedance of wire seen as a lumped parameter in an electric circuit must be made explicit. The definition is the result of some ad hoc simplifications. It depends on the way the voltage drop is defined, which is to some extent conventional. We shall use in this paper the definition of impedance (resistance and embraced flux) that is naturally suggested by the formulation (1-2) with the chosen function space for $\operatorname{grad} v$. Assuming the electrical conductivity σ is uniform per region and noting that $\beta_l = \delta_{kl}$ on Ω_{ck}, (2) can be rewritten

$$\sigma_k A_k\big(-\imath\omega\phi_k + (\Delta v)_k\big) = I_k \qquad (3)$$

and the definition of the flux embraced by the conductor,

$$\phi_k = \frac{1}{A_k}\int_{\Omega_{ck}} \mathbf{a}\cdot\mathbf{e}_z\beta_k \,\mathrm{d}\Omega_{ck} = \sum_l L_{kl} I_l \qquad (4)$$

where L_{kl} is the inductance tensor, and A_k is the cross sectional area of the given wires.

III. $\mathbf{a} - v$ Formulation with thin wires

The case of conductors idealized as thin wires with vanishing radii is now considered. They are represented by a sequence of edges of the mesh in 3D, or by nodes of the mesh in 2D, called line region in the following, and noted LR for short [2]. Equation (1) becomes in this case

$$\big(\nu\,\operatorname{curl}\mathbf{a},\,\operatorname{curl}(\alpha_n\mathbf{e}_z)\big)_\Omega - \big(I_k, \alpha_n\mathbf{e}_z\big)_{\Omega_c} = 0, \quad \forall\alpha_n \in A(\Omega). \qquad (5)$$

This idealization first implies that the flux distribution inside thin conducting regions is no longer part of the model, nor resolved by the mesh. The latter can in consequence be considerably coarser, with a substantial gain in computation time and memory space. The field distribution around thin conductors, on the other hand is still correctly represented in the model, as it only depends on the total current I_k flowing in the wire.

The geometrical idealization introduces however a representation error in the model that needs to somehow be compensated for. The analytical solution for the magnetic vector potential field around a wire with vanishing radius is indeed log-singular. As the mesh size decreases, the maximal value of the computed magnetic potential field $\mathbf{a}$ on the wire indefinitely grows in amplitude, up to values unrelated with the physical solution. Fig. 2 shows such an example of the mesh-related overestimation of the peak $\mathbf{a}$-field on a thin wire. The curve labeled “Full Model” is obtained with a fine conventional discretisation of the wire (1-2), whereas the ”LR w/o correction” is obtained with idealized conducting edges (5), Fig. 2. The orange rectangle highlights the actual radius of the wire. Note that the curves match outside the wire region.

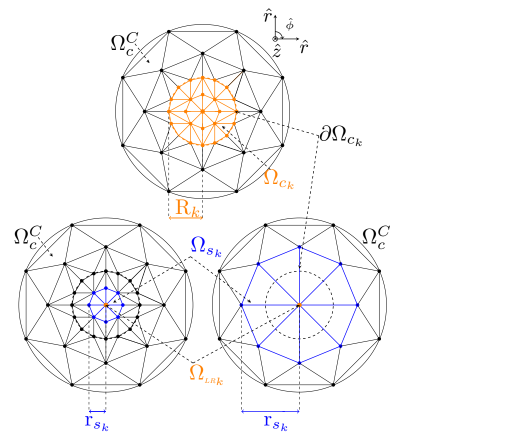

Fig. 1. Top: Mesh with explicit discretization of the real round conductor Ω_{ck} highlighted. Bottom: Mesh around the idealized (pointwise) thin conductor Ω_{LR_k} with a fine (Left) or a coarser (Right) discretization, and with highlighted mesh dependent sleeve Ω_{sk}.

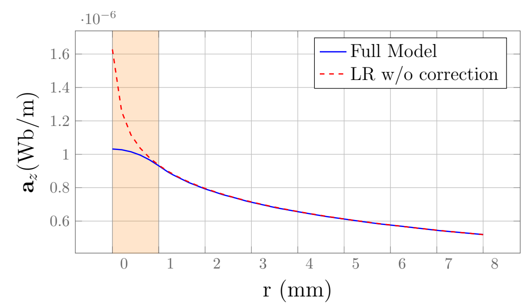

Fig. 2. Magnetic vector potential along the r-axis at 1Hz, showing the non-physical mesh-related overestimation of the peak $\mathbf{a}$-field due to the thin wire idealization compared to the physical solution obtained with the Full model.

IV. Field truncation

The proposed technique proceeds in two steps. One has to first get rid of the mesh-dependent peak introduced by the geometrical idealization, and then reintroduce in the model the internal field distribution inside the real wire by means of a known analytical solution.

We call *sleeve* the region Ω_{sk} made of the finite elements in the mesh having at least one node on Ω_{LR_k}, Fig. 1.

The shape of this region is close to a regular polygon in 2D, whose radius r_{sk} is approximately given by the prescribed mesh size at the thin wire node. In 3D, the sleeve region is cylindrical in good approximation, with a radius that may vary slowly along the wire.

The first step consists in solving an auxiliary boundary value problem, whose formulation is identical to (5), except that it is solved on the restricted region $\cup_k\Omega_{sk}$, with a homogeneous Dirichlet boundary conditions $\mathbf{a} = 0$ imposed directly on the external boundary of the sleeves, Fig. 3. We call $\mathbf{a}^c$ the solution of the initial problem (5) on Ω, and $\mathbf{a}^w$ the solution of the auxiliary problem on $\cup_k\Omega_{sk}$.

The idea behind this solving a second boundary value problem is that $\mathbf{a}^c$ and $\mathbf{a}^w$ contain the same mesh-dependent peak, because they are computed using exactly the same finite elements. The peak in the computed field $\mathbf{a}^c$ can thus

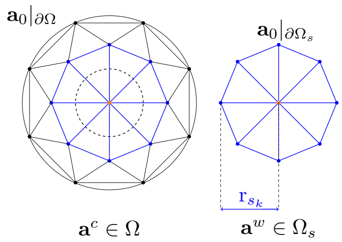

Fig. 3. Domain of analysis of the initial problem (Left), and of the auxiliary problem (Right).

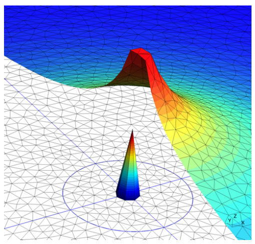

Fig. 4. Solution $\mathbf{a}^w$ of the auxiliary problem, and cut-view of truncated field $\mathbf{a}^c - \mathbf{a}^w$.

be canceled out by subtraction of $\mathbf{a}^w$. The result of the subtraction, the so called truncated field $\mathbf{a}^c - \mathbf{a}^w$, is depicted in Fig. 4. The truncated field is the sought solution of the field problem everywhere outside the sleeves $\cup_k \Omega_{sk}$. Only inside the sleeves must it be modified in order to reintroduce the details of the field distribution inside the real wire, accounting for its actual shape (round, square, rectangle) and structure (massive, coaxial, twisted).

V. Analytical correction

The general principle of the correction is a one-liner: calculate the analytical solution $\mathbf{a}_{corr}$ for the real wire carrying a current I_k with a zero-flux boundary condition imposed on the sleeve boundary. The corrected $\mathbf{a}$-field writes then simply

$$\mathbf{a} = \mathbf{a}^c - \mathbf{a}^w + \mathbf{a}_{corr}. \tag{6}$$

In order to make the analytical derivation of $\mathbf{a}_{corr}$, a number of reasonable simplifications are done in practice: the thin wire is assumed straight, the sleeve is assumed cylindrical, the analytical solution is assumed radial.

In this paper, straight massive conductors with round cross sections of radius R are considered. This allows solving the Magnetodynamics problem analytically with a 1D differential equation, in a cylindrical coordinate system aligned with the center-line of the wire, to obtain

$$\mathbf{a}_{corr}(r) = \frac{\mu_0 \hat{I}_k}{2\pi}\left(\frac{\mu_r}{\tau}\frac{J_0(\tau\frac{r}{\mathrm{R}}) - J_0(\tau)}{J_1(\tau)} + \log\left(\frac{\mathrm{r}_s}{\mathrm{R}}\right)\right)\mathbf{e}_z \tag{7a}$$

$$\mathbf{a}_{corr}(r) = \frac{\mu_0 \hat{I}_k}{2\pi}\log\left(\frac{\mathrm{r}_s}{r}\right)\mathbf{e}_z \tag{7b}$$

for $r \le \mathrm{R}$ and $\mathrm{R} < r < \mathrm{r}_s$ respectively, where $\tau = (1-\imath)\mathrm{R}/\delta$ with δ the skin depth.

The calculations have been performed with a wire radius $\mathrm{R}_k = 1\,\mathrm{mm}$, a sleeve radius (i.e., a prescribed mesh size on the wire) $\mathrm{r}_{sk} = 3\,\mathrm{mm}$, a current $\hat{I} = 1\,\mathrm{A}$, an electrical conductivity $\sigma = 5.96e7\,\mathrm{S/m}$, and a relative permeability μ_r =1. All calculations have been performed using ONELAB software (Gmsh [5] and GetDP [4]).

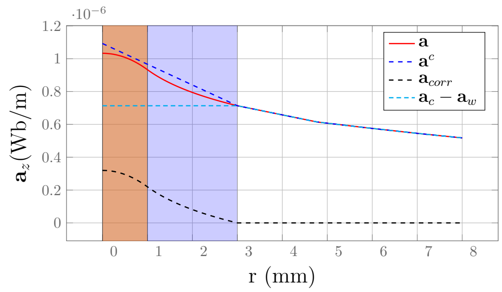

Fig. 5. Different components of the corrected field $\mathbf{a}$ as of (6).

In Fig. 5 we see the progression of the reconstruction of the $\mathbf{a}$ field, plotting the individual terms of (6). Fig. 6 shows that the corrected field (6) matches closely the field obtained by means of the conventional FE formulation with a fine discretization of the wire, both at low and high frequency.

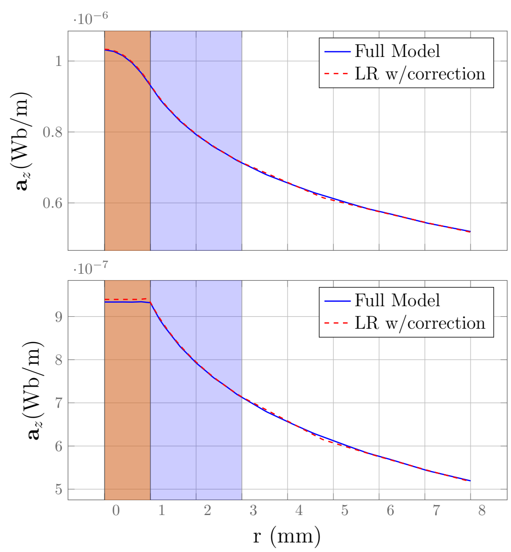

Fig. 6. Comparative view of the magnetic vector potential $\mathbf{a}$ along the r-axis for a single wire at 1Hz (Top) and 1MHz (Bottom).

The flux ϕ_k is obtained in the thin wire approach by substituting (6) into (4). As the real thin wire region is not available in the geometry in the thin wire approach, the first two terms are approximated by the value of the truncated field $\mathbf{a}^c - \mathbf{a}^w$ on the idealized wire, whereas the third term is evaluted analytically:

$$\phi_k = (\mathbf{a}^c - \mathbf{a}^w)|_{\Omega_{ck}} + \frac{\mu_0 \hat{I}_k}{2\pi}\left(\imath\mu_r\left(\frac{\delta}{R}\right)^2 - \frac{\mu_r}{\tau}\frac{J_0(\tau)}{J_1(\tau)} + \log\left(\frac{\mathrm{r}_s}{\mathrm{R}}\right)\right). \tag{8}$$

Fig. 7 shows that the proposed technique allows recovering the exact flux, and hence the exact impedance of the thin wire, with an excellent accuracy up to 1MHz, with however a significantly coarser mesh, since one has 14404 Dofs (mesh size = 0.02mm) for the Full model and only 1555 Dofs(mesh size = 3mm) for the LR model. Note that the flux obtained without correction with the same mesh is 10.925e-07 Wb.

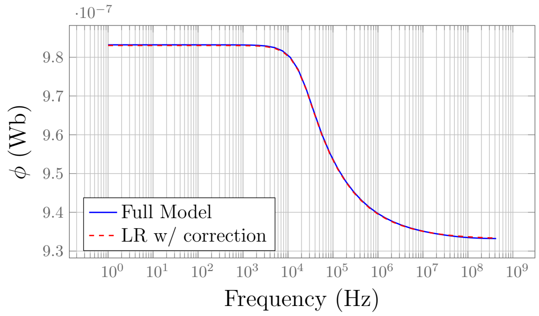

Fig. 7. Comparative view of the flux (4) vs frequency characteristic, computed with the thin wire approach and with the conventional FE method.

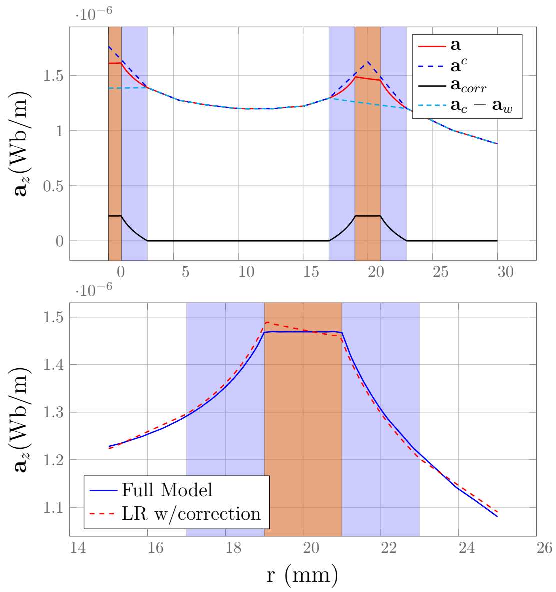

Fig. 8. Different components of the corrected field $\mathbf{a}$ as of (6) with three wires at 1MHz (Top), and comparative view of the computed $\mathbf{a}$ field focused on the rightmost wire (Bottom).

VI. Proximity effect

It has been shown in the previous section that the proposed technique is able to accurately compute the true field distribution over the whole domain of analysis and a large range of working frequencies, in the case of a single wire. One must still verify that, despite the fact that the correction is made with the analytical solution of a single wire in isolation, the effect of distant wires on a given thin wire is properly taken into consideration. A system of three equidistant thin wires is considered for this purpose. Fig. 8 (Top) shows the breakdown of the computed $\mathbf{a}$-field into the different terms of (6) at 1MHz. The flux part due to distant wires, i.e., the mutual inductance effect, is taken into account through the $\mathbf{a}^c - \mathbf{a}^w$ part. Skin effect, on the other hand, is taken into account by the correction $\mathbf{a}_{corr}$. The major limitation of our technique appears in the bottom view in Fig. 8. Eddy currents distribute asymmetrically in a wire in order to shield its interior against other current carrying conductors in the vicinity. This is the proximity effect [6], which is disregarded by our approach, as a consequence of the fact that the correction is made with the analytical solution of a single wire in isolation.

This simplification has however little impact on the accuracy of the computed flux and impedance. As one can see in Fig. 8 (Bottom), the corrected field ("LR w/ correction") is not flat in the rightmost thin wire, but the computation (8) of ϕ_k involves the value of the truncated field $\mathbf{a}^c - \mathbf{a}^w$ at the center of the wire, which is close to the exact value because the eddy currents responsible for the proximity effect are zero in average. Joule losses could however be slightly underestimated. In terms of number of unknown, one has in this case 3539 nodes and 6996 triangles for the full model, and only 1648 nodes and 3214 triangles with the thin wire technique.

VII. Conclusion

A technique for the inclusion of thin wires in FE models has been presented, one that allows a considerable reduction of the problem size with moderate loss of accuracy. It is shown that the correct impedance of the wire can be restored from an FE solution obtained with idealized thin conductors using a correction based on analytical solutions. The technique also works with more than one wire, i.e., the effect of other wires is properly taken into account despite the fact that the correction is done with the analytical solution of a single wire in isolation.

Results for a broad range of frequencies have been shown with a high degree of agreement. This method has been demonstrated for the 2D magnetodynamics case, with round massive conductors.

The extension to 3D is the subject of ongoing work as is the extension to other types of conductors, e.g. of rectangular cross section, where the analytical solution in the sleeve should be adapted accordingly. Furthermore, additional losses due to the proximity effect, which is disregarded by this approach, can sometimes be significant in practice. These losses can however be evaluated accurately in *post-processing* on the basis of the quantities computed with the finite element model with idealized wires.

References

[1] J. Jin and D. Riley, "Finite Element Analysis of Antennas and Arrays," *John Wiley and Sons*; 2009.

[2] G. Meunier, editor. "The finite element method for electromagnetic modeling", *John Wiley and Sons*, 2010.

[3] P. Dular, F. Henrotte, W. Legros. "A general and natural method to define circuit relations associated with magnetic vector potential formulations", *IEEE transactions on magnetics*, 35(3):1630-3, 1999.

[4] P. Dular, C. Geuzaine, F. Henrotte and W. Legros. "A general environment for the treatment of discrete problems and its application to the finite element method", *IEEE transactions on magnetics*, 34(5):3395–3398, 1998.

[5] C. Geuzaine and J.-F. Remacle. "Gmsh: a three-dimensional finite element mesh generator with built-in pre- and post-processing facilities", *International Journal for Numerical Methods in Engineering*, 79(11):1309-1331, 2009.

[6] J. Gyselinck and P. Dular "Frequency-domain homogenization of bundles of wires in 2-D magnetodynamic FE calculations", *IEEE transactions on magnetics*, 2005 41(5), pp.1416-1419.